Journal of Inflammation Research

Dovepress
Taylor & Francis Group

Open Access Full Text Article

ORIGINAL RESEARCH

Corn Silk Polysaccharides Before and After Selenization Reduced Calcium Oxalate Crystal-Induced HK-2 Cells Pyroptosis by Inhibiting the NLRP3-GSDMD Signaling Pathway

Jin Han[1], Xin-Yi Tong[2], Yu-Yun Zheng[2], Jia-Hui Cheng[1], Jian-Ming Ouyang[2], Ke Li[3]

[1]Department of Nephrology, The Second Affiliated Hospital, Xi'an Jiaotong University, Xi'an, People's Republic of China; [2]Institute of Biomineralization and Lithiasis Research, College of Chemistry and Materials Science; Jinan University, Guangzhou, 510632, People's Republic of China; [3]Core Research Laboratory, The Second Affiliated Hospital, Xi'an Jiaotong University, Xi'an, People's Republic of China

Correspondence: Jian-Ming Ouyang, Email toyjm@jnu.edu.cn; Ke Li, Email ke.li@mail.xjtu.edu.cn

Objective: Pyroptosis is a new type of programmed cell death associated with many inflammatory diseases. Polysaccharides have anti-inflammatory effects. In this study, we investigated whether corn silk polysaccharides (DCSP) before and after selenization (Se-DCSP) can reduce the renal tubule pyroptosis induced by calcium oxalate crystals.

Methods: HK-2 cells were exposed to calcium oxalate monohydrate with a size of 3 μm (COM-3μm) to establish a pyroptosis model. The degree of cell damage was determined by detecting cell viability, reactive oxygen species (ROS), and lactate dehydrogenase (LDH) content. The proportion of pyroptosis cells was quantitatively detected by Caspase-1/PI double staining. The expression levels of NLRP3, GSDMD, IL-18, and IL-1β were detected by confocal microscopy and Western blot analyses.

Results: DCSP and Se-DCSP can reduce the secretion of inflammatory factors IL-1β/18 related to pyroptosis by reducing cell damage and oxidative stress, as well as down-regulate the expression of Caspase-1, NLRP3, GSDMD, and TNF-α, repair damaged cells, and inhibit pyroptosis in HK-2 cells. The inhibitory effect of selenized polysaccharide was significantly enhanced compared with that before selenification.

Conclusion: Se-DCSP can inhibit pyroptosis through the NLRP3/Caspase-1/GSDMD/IL-1β/IL-18 signaling pathway to reduce the risk of kidney-stone formation.

Keywords: pyroptosis, kidney stones, calcium oxalate crystals, selenized polysaccharide

Introduction

Studies have found that calcium oxalate (CaOx) crystals deposited in renal tubules can induce mitochondria to generate excessive reactive oxygen species (ROS) and free radicals. This phenomenon mediates the activation of NOD-like receptor thermal protein domain associated protein 3 (NLRP3) inflammasome, up-regulates the expression of apoptosis-associated speck-like protein (ASC), Caspase-1 and interleukin-1β (IL-1β), and ultimately triggers renal-cell pyroptosis.[1–3] Pyroptosis primarily includes the classical pathway dependent on Caspase-1 and the non-classical pathway dependent on Caspase-4/5/11.[4] Pyroptosis can be evaluated by detecting Caspase-1 and pyroptosis-related proteins, such as NLRP3, ASC, cleaved Caspase-1, IL-1β, and IL-18.[2]

Previous studies on pyroptosis and inflammasome NLRP3 have primarily focused on the role of diseases, such as diabetes and atherosclerosis.[5] In recent years, studies have shown that pyroptosis is involved in CaOx crystalline nephropathy.[6,7] Liu et al[8] found that the pyroptosis of renal tubular epithelial cells is induced by exposure to CaOx crystals. They confirmed that extracellular adenosine triphosphate (ATP) induced by crystals can upregulate ROS generation through membrane purinergic 2 × 7 receptor and then activate IL-1β/18 maturation and gasdermin (GSDMD) cleavage mediated by NLRP3 inflammasomes. Song et al[9] found that the calcium oxalate monohydrate

Received: 30 November 2024
Accepted: 13 February 2025
Published: 12 March 2025

(COM) treatment group significantly increases the protein expression of ASC and cleaved Caspase-1 and the secretion of the pro-inflammatory factors IL-1β and interleukin-18 (IL-18). NLRP3 also plays an important role in kidney disease in animal models. For example, Sun et al[3] found that CaOx crystals can activate the TLR4/NF-κB and NLRP3 inflammasome pathways and promote the release of inflammatory mediators, leading to damage and crystal deposition in HK-2 cells and rat kidney tissues.

Blocking or inhibiting a certain link of the pyroptosis pathway can alleviate or block the process of pyroptosis, thereby inhibiting diseases related to pyroptosis. Hu et al[10] showed that disulfiram can prevent pyroptosis by preventing the formation of GSDMD pores in an inflammatory mouse model. Mannose can also inhibit Gasdermin-E (GSDME)-mediated pyroptosis by activating AMP-activated protein kinase.[11] Zhang et al[12] found that sulfonamide can act as a targeted inhibitor of GSDMD by covalently binding to the unique residue Cys191 of human GSDMD (Cys192 in mice). It also reduces the mRNA and protein levels of Caspase-1, NLRP3 inflammasome, GSDMD, and IL-1β, thereby inhibiting cell pyroptosis.

Polysaccharides can treat a variety of diseases by inhibiting pyroptosis activation. For example, Liang et al[13] showed that *Dendrobium officinale polysaccharide* can inhibit the activation of NLRP3 inflammasome, the cleavage of Caspase-1, and the production of IL-1β and IL-18, thereby inhibiting dextran sodium-induced acute colitis. Yang et al[14] showed that LBP can down-regulate the expression of NLRP3, Caspase-1, and membrane GSDMD-N. It can also improve the pyroptosis pathway in ARPE-19 cells activated by Aβ1-40, thereby inhibiting macular degeneration and protecting the retina. Wu et al[15] showed that bletilla polysaccharide can effectively reduce the release of inflammatory cytokines, inhibit the NLRP3/caspase-1/GSDMD signaling pathway, alleviate alveolar macrophage pyroptosis, and reduce the High mobility group box 1/Toll-like receptor 4 level, thereby reducing lung inflammation in acute respiratory distress syndrome mice. Corn silk polysaccharide has bioactive properties such as antioxidation, anti-inflammation and anti-glycation.[16] Meanwhile, the antioxidant and anti-inflammatory activities of corn silk polysaccharide modified by selenization are significantly enhanced. Selenium is an essential trace element in life. It plays an irreplaceable role in delaying human aging, improving immunity, preventing cardiovascular diseases and treating Keshan disease.[17] Selenopolysaccharides are organic selenium compounds that bind polysaccharides to selenium through unique chemical interactions. As a functional supplement, selenopolysaccharides are less harmful and easier to be absorbed and utilized by the human body.[18] Selenopolysaccharides have stronger biological properties than selenium and polysaccharide, including immune regulation, anti-tumor, anti-oxidation, hypoglycemic, heavy metal resistance, neuroprotection, anti-inflammation, liver protection and so on. Scientific studies have shown that selenopolysaccharides have potential for future development and have shown that it is an effective treatment for a variety of diseases.[19]

We previously prepared selenized corn silk polysaccharide (Se-DCSP) with selenium content of 1226.7 μg/g, which was much higher than that of unselenized polysaccharide DCSP (19.5 μg/g).[20] Compared with DCSP, Se-DCSP had significantly improved biological activities, including free radical scavenging ability, reducing reactive oxygen species, restoring cell viability and cell morphology, and increasing mitochondrial membrane potential. In addition, Se-DCSP could down-regulate the expression of inflammatory factors monocyte chemoattractant protein (MCP-1), NLRP3 and nitric oxide (NO) in HK-2 cells to a greater extent than DCSP. In this study, the inhibitory effect and inhibitory pathways of Se-DCSP and DCSP on pyroptosis of HK-2 cells were compared in order to provide enlightenment for reducing the risk of kidney stone formation.

Methods and Experiments

Reagents and Instruments

Reagent: Human renal proximal tubular epithelial cells (HK-2) were purchased from the Shanghai Cell Bank of the Chinese Academy of Sciences (Shanghai, China). Fetal Bovine Serum, FBS (Umedium, He Fei, China).Cell culture medium (DMEM-F12) was purchased from Haichun Biochemical Products (Beijing) Co., LTD. (Beijing, China). TNF-α, GSDMD and NLRP3 primary and secondary antibody kits were purchased from Aibo Technology Co., LTD. IL-18/IL-1β was provided by KGI Bio. Corn silk polysaccharides were provided by the Angelica species.

Instruments: Inverted fluorescence microscope (IX51, OLYMPUS, Japan); Flow cytometry (FACS Aria, BD, USA); Microplate reader (SafireZ, Tecan, Switzerland). Confocal microscope (LSM510 META DUO SCAN, ZEISS, Germany) High speed refrigerated centrifuge (Micro21R, USA).

Synthesis and Characterization of COM

COM crystals with size of 3 μm were synthesized with a slight modification according to reference.[21] The specific process is as follows: 0.04 mol/L $CaCl_2$(50 mL) was added to 300 mL secondary water, mixed evenly and water bath to 75°C, to which 0.04 mol/L Na_2Ox(50 mL) solution was added drop by drop, the reaction was kept in water bath 75°C, high-speed stirring, after the end of the drop, continue stirring for 2 min. They were left overnight at room temperature, washed twice with secondary water and once with ethanol, drained and filtered, and dried. X-ray diffraction (XRD), Fourier transform infrared spectrometer (FT-IR spectrometer) and scanning electron microscope (SEM) were performed. Crystal dimensions 100 crystals were analyzed using Nano Measurer software.

Cell Culture and Protection

Cell Viability Was Detected by CCK-8

Cells were cultured in DMEM-F12 medium with 10% fetal bovine serum (FBS) at 37°C with 5% CO_2 saturated humidity. A cell density of 1.0×10^5 cells/mL was seeded in 96-well culture plates and incubated for 24 h until the cell density was 80% for treatment. The cells were divided into 3 groups: 1) control group: serum-free medium; 2) COM damage group: containing 300 μg/mL COM-3μm; 3) Polysaccharide protection group: DCSP or Se-DCSP at concentrations of 30, 60, 90 and 120 μg/mL, and COM-3μm crystal at 300 μg/mL were added. After the above groups of cells were incubated for 48 h, the cell viability was detected according to the CCK-8 kit instructions.

Observation of Cellular ROS Levels By Laser Confocal Microscopy

Cell culture was the same as Cell Viability Was Detected by CCK8. The experiment was divided into: 1) normal group: serum-free medium; 2) COM damage group: 60 μg/mL COM-3μm was added to damage the cells for 48 h; 3) Polysaccharide protection group: 300 μg/mL COM-3μm and 60 μg/mL polysaccharide containing different selenium contents were mixed and added to the well plate. After reaching the incubation time, the old culture medium was removed by suction, washed twice with phosphate buffered saline (PBS) buffer, and 1 mL 2',7'-Dichlorodihydrofluorescein diacetate (DCFH-DA) (1:1000) diluted in serum-free culture medium was added. The cells were incubated in an incubator at 37°C containing 5% CO_2 in the dark for 30 min. After reaching the incubation time, the machine was used for observation.

Detection LDH Activity

The cell seed plate is the same as "Cell Viability Was Detected by CCK-8". The experiment was divided into the following five groups: 1) normal group: serum-free medium was added; 2) COM damage group: 60 μg/mL COM-3μm was added to damage the cells for 48 h; 3) Polysaccharide protection group: 300 μg/mL COM-3μm was mixed with 60 μg/mL polysaccharide containing different selenium content and then added to the well plate; 4) Background blank control well: no cells, only serum-free medium was added; 5) sample maximum enzyme activity control well. After reaching the predetermined time, 60 μL LDH detection working solution was added to each well and incubated in the dark for 30 min, followed by absorbance measurement at 490 nm.

Observation of Cytoskeleton By Laser Confocal Microscopy

The cell seed plate was the same as "Observation of Cellular ROS Levels By Laser Confocal Microscopy". After incubation for 24 h, cells were fixed with 4% paraformaldehyde solution for 10 min and washed 3 times × 5 min with PBS. The cells were then permeabilized for 10 min, followed by addition of Actin-tracker Green staining solution and incubation in the dark for 1 h. 4',6-diamidino-2-phenylindole (DAPI) staining solution was added and incubated in the dark for 6 min before confocal observation.

Pyroptosis Detection

Detection of the Expression of NLRP3 by Immunofluorescence

Cell seed plates and experimental groups were the same as in section "Observation of Cellular ROS Levels By Laser Confocal Microscopy". After the incubation time reached, the cells were washed three times with PBS buffer and fixed with 4% paraformaldehyde at room temperature for 30 min. After washing with PBS buffer, 0.1% Triton X-100 was added for permeabilization for 15 min, and then bovine albumin (BSA) blocking solution was added for blocking at 37°C for 2h. Then, NLRP3 rabbit Doron antibody (1:100) was added and the cells were incubated in a refrigerator at 4°C overnight, washed three times with PBS buffer, and incubated with fluorescently labeled secondary antibody at 37°C in the dark for 1 h. Finally, a small amount of DAPI staining solution was added and the cells were incubated at room temperature for 10 min. DAPI staining solution was removed by suction, and the cells were washed three times with PBS buffer. Each time was 5 min, and then the expression of NLRP3 was observed directly under the laser confocal fluorescence microscope. Semi-quantitative analysis was subsequently performed using ImageJ software.

Immunofluorescence Detection of Pore-Forming Protein GSDMD Expression

Cell culture and grouping were the same as in "Observation of Cellular ROS Levels By Laser Confocal Microscopy". Primary GSDMD antibody was added and incubated overnight at 4°C, and the other procedures were the same as in "Detection of the Expression of NLRP3 by Immunofluorescence". Image software was used for semi-quantitative analysis.

Caspase-1/PI Double Staining Was Used to Detect the Proportion of Pyroptosis Cells

Cell seeding plate and grouping were the same as in "Observation of Cellular ROS Levels By Laser Confocal Microscopy". After reaching the reaction time, the cells were digested with trypsin, resuspended in a centrifuge tube, and diluted Caspase-1 staining solution was added to incubate at 37°C for 1 h. The cells were washed with PBS three times, and propidium iodide (PI) dye was added.

The Morphology of Pyroptosis Cells Observed After Caspase-1/PI/ Hoechst 33342 Triple Staining

After reaching the action time, the culture medium was removed by suction, and the diluted Caspase-1 staining solution was added to the constant temperature incubator at 37°C for 1 h. After that, the cells were washed three times with PBS, incubated for 10 min with PI dye, washed three times with PBS, and incubated for 5 min with Hoechst 33342. Confocal microscopy was used for observation.

Detection of Caspase-1 Activity

Cell seed plates and experimental groups were the same as in "Observation of Cellular ROS Levels By Laser Confocal Microscopy". The cell culture medium was aspirated and set aside. The cells were digested with trypsin, centrifuged, collected, the supernatant discarded, and the cells washed with PBS. Two hundred microliter of lysate was added, the precipitate was resuspended, lysed in an ice bath for 15 min, centrifuged, and the supernatant was subsequently transferred to a centrifuge tube precooled in an ice bath. After the addition of Ac-YVAD-pNA (2 mm), the mixture was mixed and the absorbance was measured after incubation at 37°C for 90 min.

Detection of Intracellular Inflammatory Factors

The Expression of Tumor Necrosis Factor-α (TNF-α) and IL-6 Detected by Immunofluorescence

Cell culture and grouping were the same as in "Observation of Cellular ROS Levels By Laser Confocal Microscopy". Primary anti-TNF-α or anti-IL-6 antibodies were added and incubated overnight at 4°C with the same procedures as in "Detection of the Expression of NLRP3 by Immunofluorescence". Semi-quantitative analysis was performed with ImageJ software.

The Contents of IL-18 and IL-1β Determined by Enzyme Linked Immunosorbent Assay

Cell culture and grouping were the same as in "Observation of Cellular ROS Levels By Laser Confocal Microscopy". The levels of IL-18 and IL-1β released by the cells were quantified by enzyme linked immunosorbent assay (ELISA) kits.

The specific process is as follows: After reaching the processing time, the supernatant was sucked into a 1.5 mL centrifuge tube, centrifuged at 3000 rpm for 10 min to remove particles and polymers, then the centrifuged supernatant was added to the sample well, and then 100 μL of HRP labeled detection antibody was added. The reaction well was

sealed with a sealing plate and incubated at 37°C for 60 min. When the incubation time was reached, the liquid was discarded and pat dry on absorbent paper. Each well was filled with washing solution, left for 1 min, then the washing solution was thrown out and patted dry, and the plate was washed 5 times again. Fifty microliter of substrate A and B were added to each well and incubated at 37°C in the dark for 15 min. After that, 50 μL of termination solution was added, and the optical density (OD) value of each well was measured at 450 nm within 15 min.

Pro-IL-1β Content Determined by Western Blot

The cells were cultured in large dishes with a diameter of 12 cm and grouped as in Confocal Observation of Cellular ROS Levels. After reaching the time of action, the cells were washed with cold PBS and lysed. The lysed cells were collected and centrifuged (4°C, 15 min), and the supernatant was retained. Total protein concentrations in whole cell lysates were quantified using the BCA Protein Assay kit. The balanced protein was boiled in boiling water for 10 min until the protein was completely denatured and cooled. The amount of total protein was equal during loading, with a loading volume of 15 μL for each band of the sample. The reference protein β-tubulin was loaded on both sides of the sample and subsequently used to cut bands in a volume of 1.5 μL. Separation was performed using sodium dodecyl sulfate polyacrylamide gel electrophoresis (SDS-PAGE). Then, the isolated proteins were transferred to a 0.45 μM polyvinylidene difluoride membrane, washed three times (10 min each time) with Tris buffered saline (TBST) containing 0.2% Tween 20, blocked with 5% skim milk powder (Bio-Rad) for 2 h, and incubated with primary antibody against IL-1β overnight at 4°C. The primary antibody was recovered and washed 3 times with TBST (10 min each time). Finally, the secondary antibodies were incubated at room temperature in the dark for 2 h, washed 4 times with TBST (10 min each time), and the conjugated antibodies were visualized by a multifunctional chemiluminescence imager.

Statistical Analysis

The experimental results were statistically analyzed using the SPSS 13.0 software (SPSS Inc., Chicago, IL, USA), and the Tukey's test was used to analyze the differences between the means of each experimental group and the control group. P values less than 0.05 were considered statistically significant.

Results

Synthesis and Characterization of COM-3μm

Figure 1 shows the XRD, FT-IR and SEM images of the synthesized COM (COM-3μm) crystals. In the XRD pattern (Figure 1A), diffraction peaks with crystal-plane spacing d = 0.593, 0.365, 0.296, and 0.227 nm belonged to the (), (020), (), and (130) crystal planes of COM (PDF card number: 20–231).[21] FT-IR spectra (Figure 1B) showed that the asymmetric stretching vibration (ν_{as}) and symmetric stretching vibration (ν_s) of the carboxyl group (COO^-) of COM were 1620 and 1319 cm^{-1}, respectively. SEM images (Figure 1C) showed that COM-3μm was primarily an elongated hexagon with an average size of 3.00 ± 0.27 μm. More clarification on the COM-3μm crystals were validated and characterized and can be found in references.[21–23]

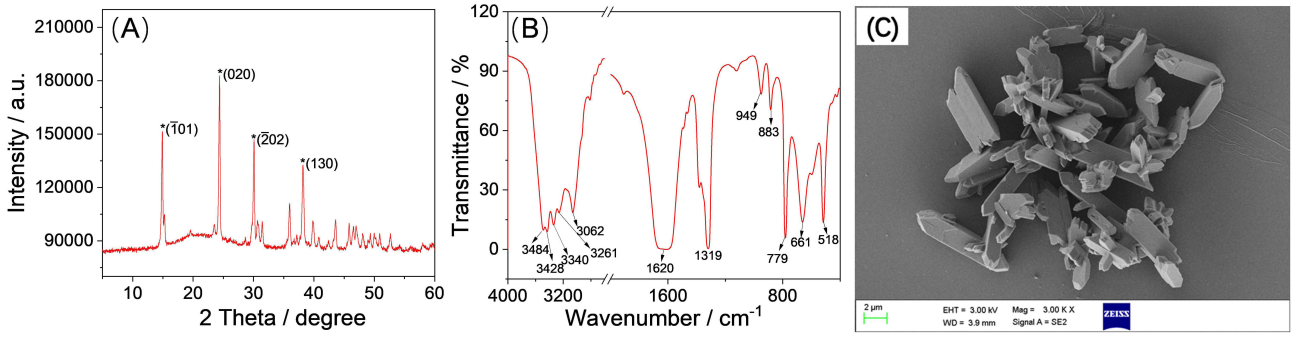

Figure 1 Synthesis and characterization of COM-3μm. (**A**) XRD pattern; (**B**) FT-IR spectrum; (**C**) SEM image.

https://doi.org/10.2147/JIR.S506093

Polysaccharide Protection Inhibited COM-3μm-Induced Oxidative Damage in Cells

Restoration of Cell Viability

COM-3μm was used to construct the pyroptosis model. The viability of HK-2 cells damaged by COM-3μm (58.9%) was significantly lower than that of the normal control group (100%) (Figure 2A). Corn silk polysaccharides before and after selenization were effective in protecting cells from COM-3μm damage. Cell viability (62.70–80.14%) significantly increased under the protection of 30, 60, 90, and 120 μg/mL DCSP or Se-DCSP compared with the COM-3μm damage group.

Se-DCSP showed greater protection than DCSP at the same concentration. When the concentration of Se-DCSP was 60 μg/mL, the cell viability of Se-DCSP and DCSP protected group was 80.1% and 71.6%, respectively.

The polysaccharide concentration is affected by the protective effect. At 60 μg/mL, polysaccharide exerted the best protective effect. In other words, too high or too low polysaccharide concentration reduced its protective ability, so 60 μg/mL polysaccharide concentration was selected for subsequent experiments.

Reduction in ROS Level

Excessive ROS may lead to cell damage. As shown in Figure 2B, cells in the injured group emitted strong green fluorescence, meaning that the ROS level was very high. The morphology of the cells shrunk, and the number of dead cells was relatively large. Conversely, cells in the normal group emitted only weak green fluorescence. After polysaccharide protection, the fluorescence intensity of cells was significantly reduced, and cell morphology improved. In particular, Se-DCSP was more effective in reducing the intracellular ROS level (Figure 2C) and oxidative stress of the cells.

Reduction in LDH Release

LDH is a marker of cell-membrane integrity and can also indicate the degree of cell damage. Figure 2D shows that the percentage of LDH released in the normal group was 8.62%, which was significantly lower than that in the injury group (33.62%). After adding polysaccharide, the release amount decreased (16.26–19.87%), among which Se-DCSP showed the best effect (16.26%).

Restoration of Cytoskeleton

Confocal laser microscopy was used to observe the changes of cytoskeleton in HK-2 cells before and after polysaccharide protection (Figure 2E). Specifically, the microfilaments of the normal group were clear and bright, with obvious protein fibers and uniform distribution around the nucleus. After crystal damage, the contraction of microfilament fibers of cells subsided and the shape was blurred, that is, the cytoskeleton was destroyed. Polysaccharide can protect the cells, thereby reversing the disappearance of microfilament fibers and restoring the basic fiber morphology of the cells. The outcome was a stronger protective effect of Se-DCSP than that of DCSP.

Polysaccharide Inhibited the Pyroptosis of HK-2 Cells

Polysaccharide Inhibited the Expression of NLRP3 and GSDMD

NLRP3 inflammasome is a multimeric protein complex formed by the innate immune sensor protein NLRP3. Excessive ROS can activate NLRP3, and the activated NLRP3 oligomerizes and binds to the adaptor protein ASC. It then recruits Caspase-1 to form NLRP3 inflammasome.[24] NLRP3 inflammasomes lead to the cleavage and activation of Caspase-1, which was further cleaved into porogenic protein GSDMD. The cleaved N-terminal fragment of GSDMD (GSDMD-N) was released to form membrane pores, thereby promoting cell pyroptosis.[25] NLRP3 (Figure 3A) and GSDMD (Figure 3C) expression in each group of cells was examined by confocal microscopy. Normal cells showed weak fluorescence, whereas HK-2 cells incubated with COM-3μm alone showed obvious green (NLRP3) or red (GSDMD) fluorescence. This finding indicated that COM-3μm injury caused an increase in the expression of NLRP3 and GSDMD. After the addition of polysaccharide protection, the fluorescence intensity of cells was weakened (Figures 3B and D), that is, the expression of NLRP3 and GSDMD was inhibited. Among these polysaccharides, Se-DCSP exhibited a better inhibitory effect than DCSP.

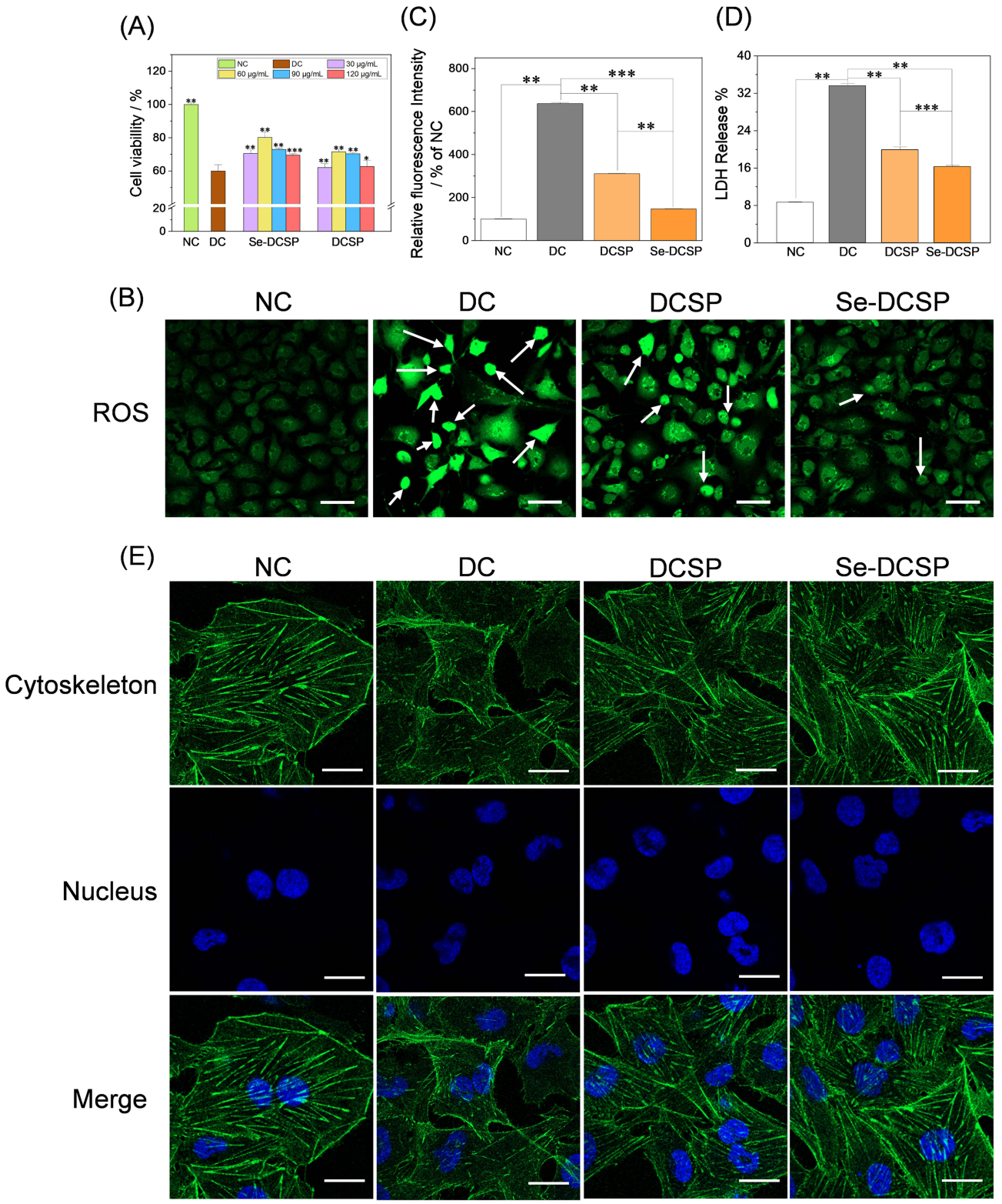

Figure 2 Protective effect of polysaccharide on HK-2 cells. (**A**) CCK8 assay was used to detect the viability of HK-2 cells. (**B**) Confocal ROS fluorescence pattern, scale: 20μm; (**C**) ROS fluorescence semi-quantitative bar graph; (**D**) LDH release. (**E**) Confocal observation of cytoskeleton, bar: 10 μm. NC: normal control group; DC: COM-3μm damage group. *P<0.05, **P<0.01, ***P<0.005. The white arrows point to cells that produce a lot of ROS.

https://doi.org/10.2147/JIR.S506093

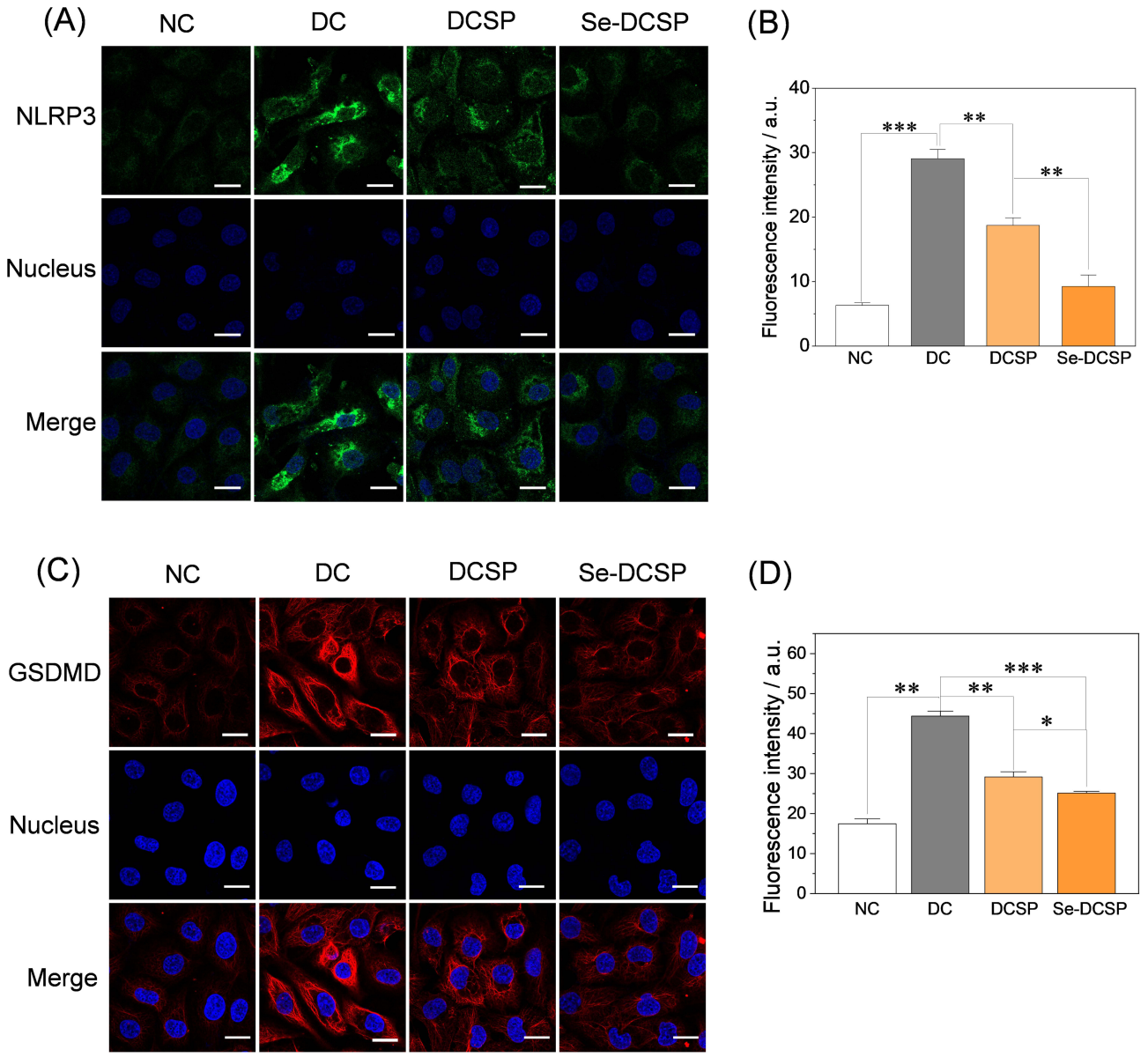

Figure 3 Detection of NLRP3 and porin GSDMD before and after polysaccharide protection. (**A**) Confocal observation of NLRP3 expression; (**B**) Semi-quantitative histogram of NLRP3 fluorescence; (**C**) Confocal observation of GSDMD expression; (**D**) Semi-quantitative histogram of GSDMD fluorescence. NC: normal control group; DC: COM-3μm damage group. *P<0.05, **P<0.01, ***P<0.005.

Polysaccharide Inhibited Pyroptosis

During pyroptosis, Caspase-1 was activated by inflammasomes (including NLRP3, NLRC4, and AIM2), which further cleaved GSDMD into GSDMD-N, released inflammatory factors such as IL-18 and IL-1β, and induced pyroptosis.[15] Accordingly, we evaluated the degree of pyroptosis by Caspase-1/PI double staining and determination of Caspase-1 content (Figure 4). As is shown in Figure 4B, the COM-3μm damdge group induced pyroptosis in 20.7% of the cells (Q2 +Q3 in Figure 4A) and apoptotic necrosis in 14.4% of the cells (Q1 in Figure 4A). After polysaccharide protection, the proportion of pyroptosis and apoptotic necrosis cells decreased. The proportion of pyroptosis cells in the Se-DCSP group decreased to 8.39%, and the proportion of apoptotic necrosis cells was 9.66%. This result suggested that Se-DCSP can inhibit COM-3μm-induced pyroptosis. The trend of cell-survival rate in each group in Figure 4A (65.71–96.44%) was consistent with the CCK-8 results (62.04–100%).

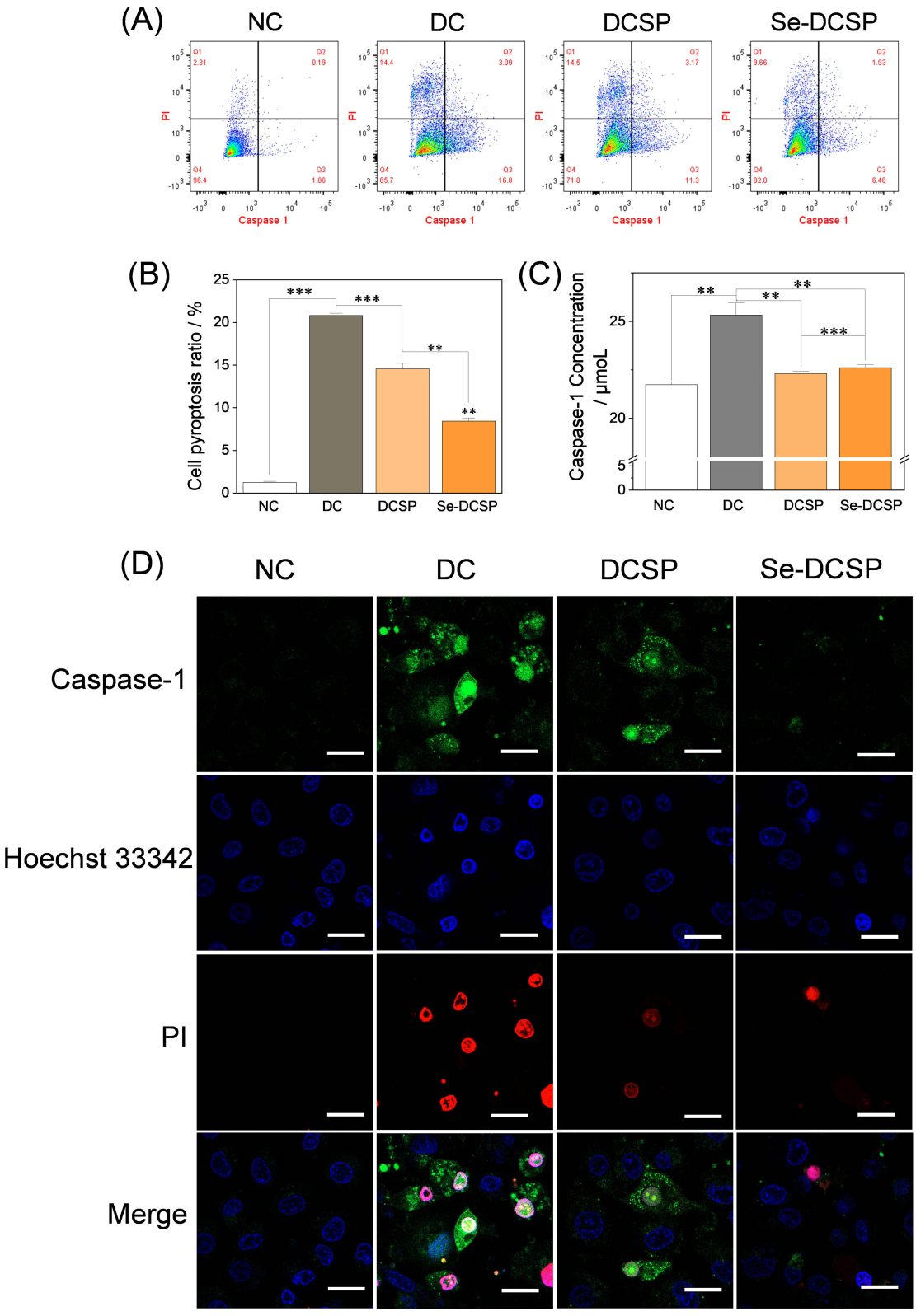

Figure 4 Pyroptosis markers in HK-2 cells treated with Se-DCSP and DCSP. (**A**) Caspase-1/PI double staining flow cytometry analysis of the proportion of pyroptosis cells; (**B**) Quantitative histogram of pyroptotic cells; (**C**) Expression of Caspase-1; (**D**) Morphology of pyroptotic cells after Caspase-1/PI/ Hoechst 33342 triple staining by confocal microscopy. NC: normal control group; DC: COM-3μm damdge group. **P<0.01, ***P<0.005. Bars: 20 μm.

https://doi.org/10.2147/JIR.S506093

The expression of Caspase-1 was also measured in the four groups of cells (Figure 4C), which was higher in the COM damege group (25.32 μmol) than in the normal control group (21.73 μmol). It was also close to the level of the normal control group in the two polysaccharide protection groups (22.30 and 22.61 μmol). These results suggested that polysaccharide can effectively reduce the number of pyroptotic cells and Caspase-1 expression.

Confocal Microscopy Used to Observe the Morphology of Pyroptosis Cells

Figure 4D shows the results of Caspase-1/PI/Hoechst 33342 triple staining observed by laser confocal microscopy. Caspase-1 fluorescent probe can penetrate cells and covalently bind to Caspase-1, showing green fluorescence signal. However, PI was blocked outside living cells and marked only the nucleus of the membrane broken cells (dead cells), showing red fluorescence. Hoechst 33342 can label the nuclei of all cells, but the blue fluorescence signal of dead cells was stronger. The differences among these three fluorescence signals can be used to distinguish normal cells, apoptotic necrotic cells, and pyroptosis cells. Cells in the normal control group in Figure 4D showed blue fluorescence, and no cells had green and red fluorescence. This finding indicated that they did not express Caspase-1, and the cell membrane was intact. Red and green fluorescence were observed in the COM damege group, indicating Caspase-1production and cell-membrane breakage. The decreased expression of green and red fluorescence in cells protected by Se-DCSP and DCSP indicated that polysaccharide reduced the expression of Caspase-1, that is, it inhibited cell pyroptosis.

Polysaccharide Reduced the Expression of Inflammatory Factors

Inhibition of TNF-α and IL-6 Expression

Tumor necrosis factor TNF-α and interleukin IL-6 are the key transcription factors involved in regulating inflammation and immune response.[26] Under normal conditions, its concentration is very low. However, it is secreted in an inflammatory environment. High concentrations of oxalate and calcium oxalate crystals can damage HK-2 cells and trigger an inflammatory response, inducing the secretion of inflammatory cytokines such as TNF-α and IL-6.[27]

TNF-α and IL-6 expression in each group was observed by confocal microscopy (Figure 5A and 5C). Normal cells showed weak fluorescence, whereas HK-2 cells incubated with COM-3μm alone showed either clear green TNF-α or red IL-6 fluorescence. This finding indicated that COM crystal injury resulted in increased TNF-α and IL-6 expression. After adding polysaccharide, the fluorescence intensity of the cells weakened (Figure 5B and D), that is, the expression of TNF-α and IL-6 was inhibited. Among these polysaccharides, Se-DCSP exhibited the best inhibitory effect.

Inhibition of Expression of the Inflammatory Factors IL-18 and IL-1β

The levels of IL-18 and IL-1β secreted by the cells were quantified using ELISA kits. The contents of IL-18 released by COM-3μm-injured cells were as high as 115.1 pg/mL, which was close to 1.5 times that of the normal control group (Figure 5E). The content of IL-1β released by the COM-3μm injury group (132.34 pg/mL) was also higher than that of the normal group (112.65 pg/mL) (Figure 5F). The contents of IL-18 and IL-1β decreased after protection with Se-DCSP. The contents of IL-18 and IL-1β decreased to 91.09 and 116.65 pg/mL, respectively, after protection with Se-DCSP. These results suggested that Se-DCSP can reduce the release of inflammatory factors to some extent.

Inhibition of Pro-IL-1β and β-Tubulin Expression

In most cells, IL-1β production requires two steps: the priming signal for precursor expression and the upstream signal molecules removed the propeptide, and then mature IL-1β was formed by cleaving Pro-IL-1β.[28] Pro-IL-1β is produced in a biologically inactive form and must undergo proteolytic cleavage to gain functional activity. However, after activation, Caspase-1 can cleave pro-IL-1β to form active IL-1β, which was secreted to the extracellular matrix.[29]

The Pro-IL-1β content was determined by Western blot, as shown in Figure 5G. In the normal control group, almost no expression of Pro-IL-1β and no obvious band was found. However, the black band in the COM damage group was obvious and higher than that in the polysaccharide protection group. The contents of β-tubulin in the four groups were similar. Semi-quantitative analysis (Figure 5H) showed that the expression of Pro-IL-1β in the DC group was 19 times higher than that in the NC group. Conversely, the Se-DCSP and DCSP protection groups were only 14 and 12 times higher than that in the NC group. Therefore, the polysaccharide can reduce the expression of Pro-IL-1β, and the effect of selenized polysaccharide was enhanced.

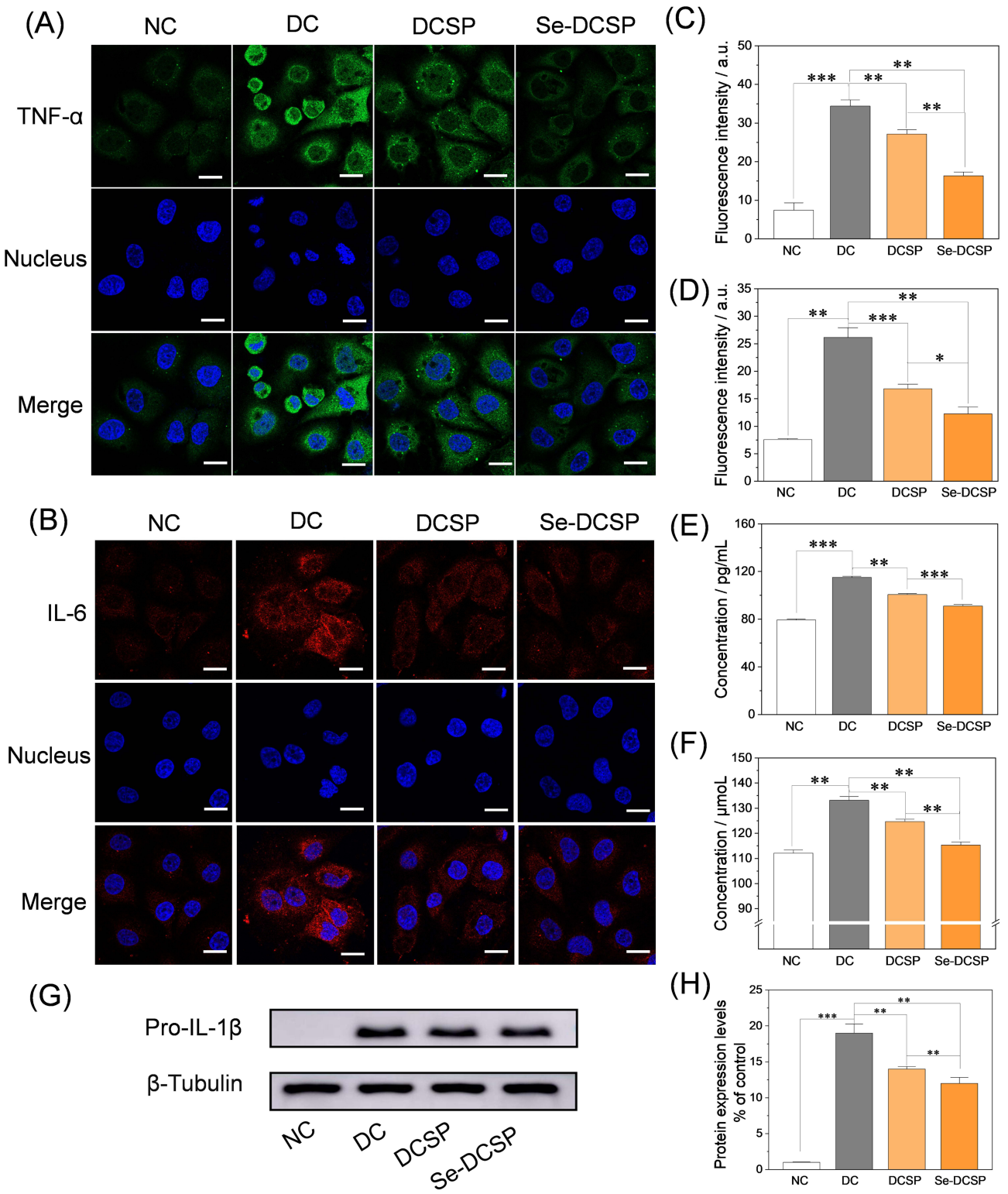

Figure 5 Inhibition of inflammatory factor expression after polysaccharide protection. (**A**) Laser confocal observation of TNF-α expression; (**B**) Semi-quantitative histogram of TNF-α fluorescence; (**C**) Laser confocal observation of IL-6 expression; (**D**) Semi-quantitative bar chart of IL-6 fluorescence; (**E**) Expression of cellular inflammatory cytokines IL-18; (**F**) Expression of cellular inflammatory cytokines IL-1β; (**G**) Protein visualization of Pro-IL-1β; (**H**) Bar chart of semi-quantitative analysis of Pro-IL-1β. NC: normal control group; DC: COM-3μm damage control group; bar: 10 μm. *P<0.05, **P<0.01, ***P<0.005.

https://doi.org/10.2147/JIR.S506093

Discussion

Inflammation and Pyroptosis in Kidney Stones

CaOx crystal deposition can cause inflammation and attract many inflammatory cells, including leukocytes, monocytes, and macrophages. Studies[30] have shown that urinary inflammatory markers (such as macrophage inflammatory protein-1β and IL-13) were higher in patients with stones than in healthy controls. Anders et al[31] found in an animal study that NLRP3 inflammasome plays an important role in the progression of nephrocalcinosis related chronic kidney disease. Inhibiting the formation of NLRP3 inflammasome by β-hydroxybutyrate can reduce ASC oligomerization. It also reduces the mRNA expression of kidney injury marker in mouse kidney, thereby reducing renal tubular injury.

As a form of programmed cell death, pyroptosis is primarily triggered by the activation of the related Caspase family by NLRP3 inflammasome and the subsequent formation of membrane pores by cleaved GSDMD.[32] Ding et al[7] conducted in vivo experiments to study the expression of pyroptosis-related proteins. Compared with control mice, vitexin administration leads to a significant reduction in the expression of IL-1β and GSDMD in renal tubular epithelium, and can reduce the expression of crystal adhesion-related molecules osteopontin and CD44. This phenomenon helps reduce crystal adhesion. Similarly, NLRP3 accelerates glomerulosclerosis in a mouse model of CaOx nephropathy and causes progressive renal failure by mediating an inflammatory response.[33]

Signaling Pathways in Pyroptosis Models

In most studies in the field of kidney stones, pyroptosis models are basically established through the damage of calcium oxalate crystals. For example, Ding[7] established a mouse model of kidney stones induced by glyoxylate and a cell model of renal tubular epithelial cells and macrophages treated with COM. Liu[8] induced the pyroptosis of renal tubular epithelial cells using synthetic CaOx crystals. COM crystals, the main form of calcium oxalate, are also much more damaging to cells than calcium oxalate dihydrate.[34] Therefore, in the current work, HK-2 cells were damaged by COM with a size of 3 μm to construct a pyroptosis model.

Numerous studies have shown that HK-2 cells can produce a large amount of ROS under COM oxidative stress, and ROS can activate NLRP3 inflammasome. ROS inhibitors can block the activation of NLRP3 inflammasome, alleviate cellular inflammatory damage, and delay the formation of kidney stones.[35] For example, Gan et al[36] treated HK-2 with CaOx crystals. They found that the levels of LDH and malondialdehyde increased, the level of superoxide dismutase (SOD) decreased, and the expression of activated Caspase-1, IL-18, and IL-1β increased. This finding indicated that CaOx crystals can aggravate the pyroptosis of HK-2 cells. Studies[37] have found that CaOx crystals can activate the NLRP3/ASC/Caspase-1 signaling pathway in mononuclear phagocytes, initiate IL-1β-dependent innate immunity, cause renal tubular damage, and promote the progression of CaOx nephropathy in mice. The TLR-4/NF-κB signaling pathway also activates monocytes and macrophages to produce a large number of inflammatory factors such as IL-6 and TNF-α, causing cell damage and promoting the formation of kidney stones.

Herein, the levels of NLRP3 and GSDMD in normal HK-2 cells significantly increased after COM-3μm injury, which induced the secretion of the downstream inflammatory factors IL-18 and IL-1β. The levels of IL-6 and TNF-α also further increased. The reason may be that cells produced oxidative stress response after injury, resulting in increased ROS content and activated NLRP3 inflammasome. Accordingly, cell pyroptosis was mediated, and inflammatory factors were secreted, consistent with the study of Tian et al.[1]

Polysaccharides Inhibited Pyroptosis and Reduced the Risk of Kidney-Stone Formation

How to specifically inhibit pyroptosis and reduce the risk of kidney-stone formation has great significance. Fang et al[38] showed that lycopene significantly improves CaOx crystal deposition, rescues renal function, and inhibits renal injury by reducing oxidative stress and pyroptosis in rats. As biomolecules, polysaccharides have regulatory effects on signaling molecules such as NF-κB, NLRP3, and ROS. However, further studies are needed to determine whether polysaccharides can inhibit pyroptosis by affecting related signaling pathways.[39] *Pachymia cocos* can reportedly inhibit NLRP3-mediated pyroptosis and alleviate the damage to the small-intestinal barrier.[40] *Lycium barbarum polysaccharide* can significantly improve liver injury owing to non-alcoholic steatohepatitis by inhibiting the NLRP3/6 inflammatory pathway and NF-κB

activation. The outcome is increased serum alanine aminotransferase and aspartate aminotransferase levels.[41] Fucoidan can reduce the expression of inflammasome NLRP3 in gastric ulcer tissue and can reduce the expression of the pyroptosis markers Caspase-1, Caspase-11, NLRP3, and Gasdermin D. The level of IL-18 also decreases significantly ($p < 0.05$).[42] *Polygonum polysaccharide* inhibits pyroptosis through NLRP3/GSDMD signaling and has a potential protective effect on SALI in septic acute liver injury. This is reflected in the reduced liver-function indicators AST, ALT, ALP, and TBIL, as well as the inflammatory cytokines TNF-α and IL-6 in serum. The levels of inflammatory cytokines IL-18 and IL-1β are related to pyroptosis.[43] Our results showed that polysaccharides inhibited pyroptosis through the NLRP3/Caspase-1/GSDMD/IL-1β/IL-18 signaling pathway (Figure 6).

The inhibitory effect of Se-DCSP was better than that of DCSP. The reason may be that selenium addition weakened the hydrogen-bond dissociation energy and enhanced the hydrogen supply capacity, thereby improving the antioxidant activity of polysaccharides.[44] The ROS production was further reduced, and the secretion of inflammatory factors such as IL-6 and TNF-α was down-regulated. Thus, the risk of kidney-stone formation was reduced.

Different crystal types, concentrations, morphologies, and sizes lead to tubular cell injury by modulating different forms of cell death. CaOx stone is considered to be a metabolic disorder, and cell death and stone development are closely related.[45] Pyroptosis promotes the development of kidney stone by damaging the integrity of cell membrane and promoting crystal adhesion.[46] Many compounds for the prevention and treatment of CaOx stone have been developed based on the anti-inflammatory and antioxidant activities of materials.[47,48] Se-DCSP not only has anti-inflammatory and antioxidant activities,[20] but also inhibits inflammation by inhibiting pyroptosis induced by the NLRP3-GSDMD pathway. Therefore, Se-DCSP has a potential effect in the prevention and treatment of kidney stones.

Conclusions

Most studies on kidney stones have focused on the oxidative damage of calcium oxalate crystals to HK-2 cells, as well as the apoptosis and necrosis caused by calcium oxalate crystals. Few reports have been made about calcium oxalate

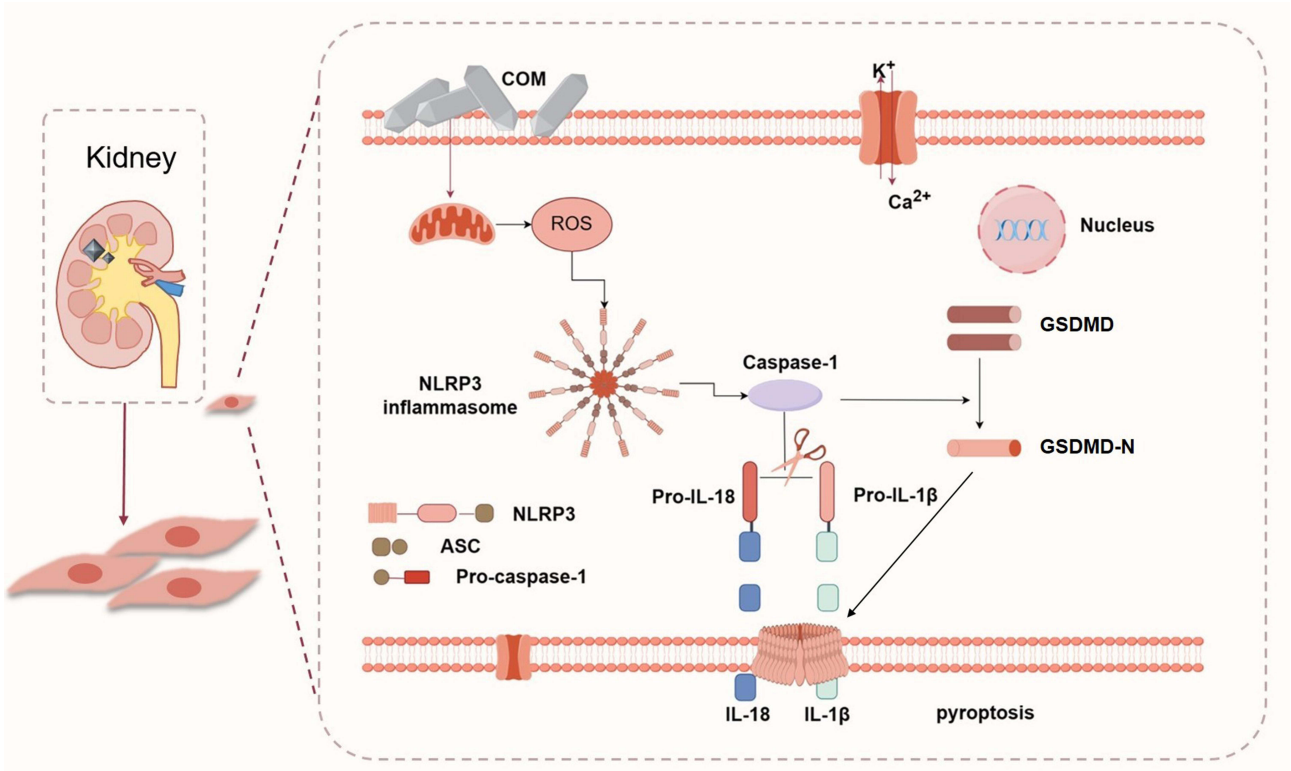

Figure 6 Se-DCSP inhibits pyroptosis through the NLRP3/Caspase-1/GSDMD/IL-1β/IL-18 signaling pathway. (By Figdraw).

https://doi.org/10.2147/JIR.S506093

crystals inducing pyroptosis and causing renal injury. In this work, COM-3μm was successfully used to induce pyroptosis. Corn silk polysaccharide inhibited pyroptosis to a certain extent by reducing ROS production and down-regulating the expression of NLRP3 inflammasome, GSDMD, and Caspase-1. Se-DCSP showed stronger biological activity. It reduced the secretion of TNF-α, IL-6, IL-18, and IL-1β to a greater extent and thus avoided the expansion of the inflammatory cascade reaction. Se-DCSP can reduce calcium oxalate-induced renal tubule pyroptosis by inhibiting the NLRP3/Caspase-1/GSDMD/IL-1β/IL-18 signaling pathway, which reduced the risk of kidney-stone formation. In the future, more cell line studies and in vivo experiments are needed to further investigate the therapeutic effect of Se-DCSP on kidney stones.

Statement of Human and Animal Rights

This article does not contain any studies with human and animal subjects performed by any of the authors.

Data Sharing Statement

All the data supporting the results were shown in the study and can be applicable from the corresponding author.

Ethical Statement

Not applicable. There were no human subjects. There were no animal subjects.

Acknowledgments

This work was supported by the National Natural Science Foundation of China (Nos. 82270800, 82400865) and Zhongguancun Nephrology & Blood Purification Innovation Alliance (NBPIA20QC0201).

Disclosure

The authors declare that they have no conflicts of interest in this work.

References

1. Tian W, Wang Z, Tang -N-N, et al. Ascorbic acid sensitizes colorectal carcinoma to the cytotoxicity of arsenic trioxide via promoting reactive oxygen species-dependent apoptosis and pyroptosis. *Front Pharmacol*. 2020;123 10: 3389.
2. Cocco M, Garella D, Di Stilo A, et al. Electrophilic warhead-based design of compounds preventing NLRP3 inflammasome-dependent pyroptosis. *J Med Chem*. 2014;57(24):10366–10382. doi:10.1021/jm501072b
3. Sun Y, Liu Y, Guan X, et al. Atorvastatin inhibits renal inflammatory response induced by calcium oxalate crystals via inhibiting the activation of TLR4/NF-κB and NLRP3 inflammasome. *IUBMB Life*. 2020;72(5):1065–1074. doi:10.1002/iub.2250
4. Tsuchiya K. Switching from apoptosis to pyroptosis: gasdermin-elicited inflammation and antitumor immunity. *Int J mol Sci*. 2021;22(1):426. doi:10.3390/ijms22010426
5. Shao F. Gasdermins: making pores for pyroptosis. *Nat Rev Immunol*. 2021;21(10):620–621. doi:10.1038/s41577-021-00602-2
6. Hou Y, Wang Q, Han B, Chen Y, Qiao X, Wang L. CD36 promotes NLRP3 inflammasome activation via the mtROS pathway in renal tubular epithelial cells of diabetic kidneys. *Cell Death Dis*. 2021;12(6):1–16. doi:10.1038/s41419-021-03813-6
7. Ding T, Zhao T, Li Y, et al. Vitexin exerts protective effects against calcium oxalate crystal-induced kidney pyroptosis in vivo and in vitro. *Phytomedicine*. 2021;86:153562. doi:10.1016/j.phymed.2021.153562
8. Liu J, Yang K, Jin Y, et al. H3 relaxin protects against calcium oxalate crystal-induced renal inflammatory pyroptosis. *Cell Proliferat*. 2020;53(10): e12902. doi:10.1111/cpr.12902
9. Song Z, Zhang Y, Gong B, Xu H, Hao Z, Liang C. Long noncoding RNA LINC00339 promotes renal tubular epithelial pyroptosis by regulating the miR-22-3p/NLRP3 axis in calcium oxalate–induced kidney stone. *J Cell Biochem*. 2019;120(6):10452–10462. doi:10.1002/jcb.28330
10. Hu JJ, Liu X, Xia S, et al. FDA-approved disulfiram inhibits pyroptosis by blocking gasdermin D pore formation. *Nat Immunol*. 2020;21 (7):736–745. doi:10.1038/s41590-020-0669-6
11. Ai Y, Wang W, Liu F, et al. Mannose antagonizes GSDME-mediated pyroptosis through AMPK activated by metabolite GlcNAc-6P. *Cell Res*. 2023;33(12):904–922. doi:10.1038/s41422-023-00848-6
12. Zhang J, Wei K. Necrosulfonamide reverses pyroptosis-induced inhibition of proliferation and differentiation of osteoblasts through the NLRP3/caspase-1/GSDMD pathway. *Exp Cell Res*. 2021;405(2):112648. doi:10.1016/j.yexcr.2021.112648
13. Liang J, Chen S, Chen J, et al. Therapeutic roles of polysaccharides from Dendrobium Officinaleon colitis and its underlying mechanisms. *Carbohyd Polym*. 2018;185:159–168. doi:10.1016/j.carbpol.2018.01.013
14. Yang M, So K-F, Lo ACY, Lam WC. The effect of Lycium barbarum polysaccharides on pyroptosis-associated amyloid β1-40 oligomers-induced adult retinal pigment epithelium 19 cell damage. *Int J mol Sci*. 2020;21(13):4658. doi:10.3390/ijms21134658
15. Wu Q, Zhou M, Chen Y, et al. Bletilla striata polysaccharides protect against ARDS by modulating the NLRP3/caspase1/GSDMD and HMGB1/TLR4 signaling pathways to improve pulmonary alveolar macrophage pyroptosis. *J Ethnopharmacol*. 2024;319:117361. doi:10.1016/j.jep.2023.117361

16. Pan Y, Wang C, Chen Z, Li W, Yuan G, Chen H. Physicochemical properties and antidiabetic effects of a polysaccharide from corn silk in high-fat diet and streptozotocin-induced diabetic mice. *Carbohyd Polym*. 2017;164:370–378. doi:10.1016/j.carbpol.2017.01.092
17. Yang WJ, Huang GL, Chen F, Huang HL. Extraction/synthesis and biological activities of selenopolysaccharide. *Trends Food Sci Technol*. 2021;109:211–218. doi:10.1016/j.tifs.2021.01.028
18. Qi Z, Duan A, Ng K. Selenosugar, selenopolysaccharide, and putative selenoflavonoid in plants. *Compr Rev Food Sci Food Saf*. 2024;23(3): e13329. doi:10.1111/1541-4337.13329
19. Chang MW, Liu KL. Selenium-polysaccharide: structural and physical characterization, bioactivities and application. *Food Rev Int*. 2024;40 (10):3291–3314. doi:10.1080/87559129.2024.2348090
20. Zheng -Y-Y, Tong X-Y, Zhang D-Y, Ouyang J-M. Enhancement of antioxidative and anti-inflammatory activities of corn silk polysaccharides after selenium modification. *J Inflamm Res*. 2024;17:7965–7991. doi:10.2147/JIR.S467665
21. Sun XY, Ouyang JM, Liu AJ, Ding YM, Gan QZ. Preparation, characterization, and in vitro cytotoxicity of COM and COD crystals with various sizes. *Mater Sci Eng C*. 2015;57:147–156. doi:10.1016/j.msec.2015.07.032
22. Nong WJ, Tong XY, Ouyang JM. Comparison of endoplasmic reticulum stress and pyroptosis induced by pathogenic calcium oxalate monohydrate and physiologic calcium oxalate dihydrate crystals in HK-2 cells: insights into kidney stone formation. *Cells*. 2024;13(24):2070. doi:10.3390/cells13242070
23. Sun XY, Ouyang JM, Gan QZ, Liu AJ. Renal epithelial cell injury induced by calcium oxalate monohydrate depends on their structural features: size, surface, and crystalline structure. *J Biomed Nanotechnol*. 2016;12(11):2001–2014. doi:10.1166/jbn.2016.2289
24. Lamkanfi M, Dixit VM. Mechanisms and functions of inflammasomes. *Cell*. 2014;157(5):1013–1022. doi:10.1016/j.cell.2014.04.007
25. Sborgi L, Rühl S, Mulvihill E, et al. GSDMD membrane pore formation constitutes the mechanism of pyroptotic cell death. *EMBO J*. 2016;35 (16):1766–1778. doi:10.15252/embj.201694696
26. Dong X, Swaminathan S, Bachman LA, Croatt A-J, Nath K-A, Griffin M-D. Resident dendritic cells are the predominant TNF-secreting cell in early renal ischemia–reperfusion injury. *Kidney Int*. 2007;71(7):619–628. doi:10.1038/sj.ki.5002132
27. Xiong P, Zheng YY, Ouyang JM. Carboxylated Pocoa polysaccharides inhibited oxidative damage and inflammation of HK-2 cells induced by calcium oxalate nanoparticles. *Biomed Phar*. 2023;169:115865. doi:10.1016/j.biopha.2023.115865
28. Li Y, Jiang Q. Uncoupled pyroptosis and IL-1β secretion downstream of inflammasome signaling. *Front Immunol*. 2023;14:1128358. doi:10.3389/fimmu.2023.1128358
29. Kwak A, Lee Y, Kim H, Kim S. Intracellular interleukin (IL)-1 family cytokine processing enzyme. *Arch Pharm Res*. 2016;39(11):1556–1564. doi:10.1007/s12272-016-0855-0
30. Kusumi K, Ketz J, Saxena V, Spencer JD, Safadi F, Schwaderer A. Adolescents with urinary stones have elevated urine levels of inflammatory mediators. *Urolithiasis*. 2019;47(5):461–466. doi:10.1007/s00240-019-01133-1
31. Anders HJ, Suarez-Alvarez B, Grigorescu M. The macrophage phenotype and inflammasome component NLRP3 contributes to nephrocalcinosis-related chronic kidney disease independent from IL-1–mediated tissue injury. *Kidney Int*. 2018;93(3):656–669. doi:10.1016/j.kint.2017.09.022
32. Tonnus W, Linkermann A. Gasdermin D and pyroptosis in acute kidney injury. *Kidney Int*. 2019;96(5):1061–1063. doi:10.1016/j.kint.2019.07.002
33. Knauf F, Asplin JR, Granja I, et al. NALP3-mediated inflammation is a principal cause of progressive renal failure in oxalate nephropathy. *Kidney Int*. 2013;84(5):895–901. doi:10.1038/ki.2013.207
34. Guerra A, Ticinesi A, Allegri F, Pinelli S, Aloe R, Meschi T. Idiopathic calcium nephrolithiasis with pure calcium oxalate composition: clinical correlates of the calcium oxalate dihydrate/monohydrate (COD/COM) stone ratio. *Urolithiasis*. 2020;48(3):271–279. doi:10.1007/s00240-019-01156-8
35. Yu X, Lan P, Hou X, et al. HBV inhibits LPS-induced NLRP3 inflammasome activation and IL-1β production via suppressing the NF-κB pathway and ROS production. *J Hepatol*. 2017;66(4):693–702. doi:10.1016/j.jhep.2016.12.018
36. Gan XG, Wang ZH, Xu HT. Mechanism of miRNA-141-3p in calcium oxalate-induced renal tubular epithelial cell injury via NLRP3-mediated pyroptosis. *Kidney Blood Press R*. 2022;47(5):300–308. doi:10.1159/000521795
37. Mulay SR, Kulkarni OP, Rupanagudi KV. Calcium oxalate crystals induce renal inflammation by NLRP3-mediated IL-1β secretion. *J Clin Invest*. 2013;123(1):236–246. doi:10.1172/JCI63679
38. Fang Z, Zheng K, Gao X. Lycopene from tomatoes and tomato products exerts renoprotective effects by ameliorating oxidative stress, apoptotic, pyroptotic, fibrotic, and inflammatory injury in calcium oxalate nephrolithiasis: underlying mechanisms. *Food Funct*. 2024;10: 1039.
39. Fan W, Lü K, Wu C, Jin ZY, Jiang Y, Song H. Progress in research on cell pyroptosis and the potential role of polysaccharides in regulating it. *Food Sci*. 2022;11:345–354.
40. Ye H, Ma S, Qiu Z, et al. Poria cocos polysaccharides rescue pyroptosis-driven gut vascular barrier disruption in order to alleviates non-alcoholic steatohepatitis. *J Ethnopharmacol*. 2022;296:115457. doi:10.1016/j.jep.2022.115457
41. Xiao J, Wang F, Liong EC, So K-F, Tipoe GL. Lycium barbarum polysaccharides improve hepatic injury through NFkappa-B and NLRP3/6 pathways in a methionine choline deficient diet steatohepatitis mouse model. *Int J Biol Macromol*. 2018;120:1480–1489. doi:10.1016/j.ijbiomac.2018.09.151
42. Selim HM, Negm WA, Hawwal MF, et al. Fucoidan mitigates gastric ulcer injury through managing inflammation, oxidative stress, and NLRP3-mediated pyroptosis. *Int Immunopharmacol*. 2023;120:110335. doi:10.1016/j.intimp.2023.110335
43. Xiao L, Qi L, Zhang G, et al. Polygonatum sibiricum polysaccharides attenuate lipopoly-saccharide-induced septic liver injury by suppression of pyroptosis via NLRP3/GSDMD signals. *Molecules*. 2022;27(18):5999. doi:10.3390/molecules27185999
44. Wang J, Hu S, Nie S, Yu Q, Xie M. Reviews on mechanisms of in vitro antioxidant activity of polysaccharides. *Oxid Med Cell Long*. 2016;2016:5692852. doi:10.1155/2016/5692852
45. Wu L, Xue X, He C, Lai Y, Tong L. Cell death-related molecules and targets in the progression of urolithiasis (Review). *Int J Mol Med*. 2024;53 (6):52. doi:10.3892/ijmm.2024.5376
46. Chen Y, Yang S, Kong H, et al. Oxalate-induced renal pyroptotic injury and crystal formation mediated by NLRP3-GSDMD signaling in vitro and in vivo. *Mol Med Rep*. 2023;28(5):209. doi:10.3892/mmr.2023.13096
47. Salem PPO, Silva DO, Silva PRS, et al. Bioguided isolation of anti-inflammatory and anti-urolithiatic active compounds from the decoction of Cissus gongylodes leaves. *J Ethnopharmacol*. 2025;337(Pt 3):118950. doi:10.1016/j.jep.2024.118950
48. Sun Y, Sun H, Zhang Z, et al. New insight into oxidative stress and inflammatory responses to kidney stones: potential therapeutic strategies with natural active ingredients. *Biomed Pharmacother*. 2024;179:117333. doi:10.1016/j.biopha.2024.117333